References

[1] Mayers, J. and Wrenn, B. G., "Combined Influence of Higher-Order Linear Effects and Nonlinear Effects on the Lateral Vibration Behavior of Solid and Sandwich Beams," SUDAER 208, Sept. 1964, Stanford Univ. Dept. of Aeronautics and Astronautics.

[2] Srinivasan, A. V., "Large Amplitude-Free Oscillations of Beams and Plates," *AIAA Journal*, Vol. 3, No. 10, Oct. 1965, pp. 1951–1953.

[3] Evensen, D. A., "Nonlinear Vibrations of Beams with Various Boundary Conditions," *AIAA Journal*, Vol. 6, No. 2, Feb. 1968, pp. 370–372.

[4] Ray, J. D. and Bert, C. W., "Nonlinear Vibrations of a Beam with Pinned Ends," *Transactions of the American Society of Mechanical Engineers* (*Journal of Engineering for Industry*), Nov 1969, pp. 997–1004.

[5] Woinowsky-Krieger, S., "The Effect of an Axial Force on the Vibration of Hinged Bars," *Journal of Applied Mechanics*, Vol. 17, No. 1, March 1950, pp. 35–36.

[6] Burgreen, D., "Free Vibrations of a Pin-Ended Column with Constant Distance Between the Pin Ends," *Journal of Applied Mechanics*, Vol. 18, No. 2, June 1951, pp. 135–139.

[7] Eringen, A. C., "On the Nonlinear Vibration of Elastic Bars," *Quarterly of Applied Mathematics*, Vol. 10, 1952, pp. 361–369.

[8] Chu, H. N. and Herrmann, G., "Influence of Large Amplitudes on Free Flexural Vibrations of Rectangular Elastic Plates," *Journal of Applied Mechanics*, Vol. 23, 1956, pp. 532–540.

[9] Chu, H. N., "Influence of Transverse Shear on Nonlinear Vibrations of Sandwich Beams with Honeycomb Cores," *Journal of the Aerospace Sciences*, Vol. 28, 1961, pp. 405–410.

[10] Young, D. and Felgar, R. P., "Table of Characteristic Functions Representing Normal Modes of Vibration of a Beam," Publication 4913, July 1949, Univ. of Texas, Austin, Texas.

[11] Felgar, R. P., "Formulas for Integrals Containing Characteristic Functions of a Vibrating Beam," Circular 14, 1950, Bureau of Engineering Research, Univ. of Texas, Austin, Texas.

[12] Herrmann, G., "Influence of Large Amplitude on Flexural Motions of Elastic Plates," TN 3578, 1956, National Advisory Committee for Aeronautics.

Shape and Surrounding Flowfield of a Drop in a High-Speed Gas Stream

A. A. Ranger*
Purdue University, Lafayette, Ind.

AND

J. A. Nicholls†
The University of Michigan, Ann Arbor, Mich.

Nomenclature

a = ellipse semimajor axis
b = ellipse semiminor axis
c = constant = $(a^2 - b^2)^{1/2}$
C_p = pressure coefficient = $(p - p_\infty)/(\frac{1}{2}\rho_\infty V_\infty^2)$
e = constant = $[1 - (b/a)^2]^{1/2}$
f = $c \sinh \xi$
k = constant = $e(1 - e^2)^{1/2} - \sin^{-1} e$
p = static pressure
r = polar coordinate (radial)
V = flowfield velocity
x = $c \sinh\xi \cos\eta$
y = $c \cosh\xi \sin\eta$
ζ = complex variable = $\xi + i\eta$
θ = polar coordinate (azimuthal)
Φ = velocity potential
ρ = fluid density

Subscripts

0 = droplet surface
∞ = undisturbed freestream conditions

Superscripts

$(\ )'$ = differentiation *wrt* ζ
$(\bar{\ })$ = complex conjugate

Received May 18, 1970; revision received June 10, 1970. The work reported here was conducted under NASA Contract NASr 54(07).

* Assistant Professor, School of Aeronautics, Astronautics, and Engineering Sciences. Member AIAA.

† Professor, Department of Aerospace Engineering. Associate Fellow AIAA.

Introduction

WHEN a spherical liquid droplet is introduced into a convective gas stream it is observed to be flattened out in such a way as to present its largest dimension in a direction perpendicular to the oncoming flow.[1] The deformation that the drop undergoes is caused by the aerodynamic forces at the surface. The action of these external forces is opposed by the surface tension forces the inertial forces, and, to a lesser extent, by the viscous forces of the liquid. If the external forces are strong enough to overcome the internal restraining forces, the drop becomes unstable and disintegrates. The mechanism and speed of the ensuing breakup process depend on how much the aerodynamic pressure forces exceed the minimum value required to produce instability. If the pressure forces are just slightly larger than the minimum value necessary for fragmentation, the mechanism of breakup is the bag type.[2] On the other hand, if the aerodynamic forces far exceed the critical value, the disintegration appears to result from a boundary-layer stripping phenomenon.[3] It is the latter mechanism which has been observed to prevail in a high-speed gas stream.

The high-speed shattering of a droplet was first modeled analytically by G. I. Taylor[4] who assumed that the drop was squashed into a plano-convex lenticular shape before having its surface stripped away by the viscous shearing forces of the surrounding air stream. As a consequence of this assumption that the windward surface is spherical and the leeward one is planar, the diameter of the flattened drop was found to be approximately one and a half times larger than the initial diameter. However, an analysis of the photographic results of Ranger and Nicholls[5] indicates that the flattened drop has a maximum diameter that is appreciably greater than one and a half times the original, and that the shape of its windward surface is actually ellipsoidal. Unfortunately, it is impossible to ascertain from the photographs the shape of the leeward surface because it is completely obscured from view by a dense region of micromist being shed continuously from the droplet equator into its wake. The importance of these observations lies in the fact that the character of the flowfield surrounding a disintegrating droplet is quite different from that assumed by Taylor. In particular, the flow over the windward surface will be greatly influenced by the degree to which that surface deviates from being spherical. Thus, the purpose of the analysis that follows is to assess the influence of droplet shape on the velocity and pressure distributions over the windward surface of a drop in a high-speed gas stream. Flowfield calculations for this shape are not available in the literature.

Analysis

It has been established from experiment[5] that when a spherical liquid drop is introduced into a gas stream it responds to the attendant aerodynamic forces by deforming into a new shape closely resembling that of a planetary ellipsoid.‡ Naturally, any alteration in shape of the droplet will produce concurrent changes in the external flowfield around the drop, and vice versa, because the shape that the drop assumes and

‡ A planetary ellipsoid, which is also known as an oblate spheroid, is the body generated by rotating an ellipse about its minor axis.

the streamline pattern of the surrounding flowfield are inextricably coupled together through the boundary conditions at the interface. Thus, the object of the analysis is to obtain a parametric solution for the external flowfield around a deforming droplet with the drop shape or eccentricity as the free parameter.

Let us consider the streaming motion of an ideal, irrotational fluid past a planetary ellipsoid as depicted schematically in Fig. 1. The motion is found by superimposing a uniform flow ($-V_\infty$) on a solution given in Ref. 6. The superposition is accomplished by adding the respective velocity potentials together.

If the potential function for the uniform stream $-V_\infty$; i.e.,

$$\Phi = xV_\infty$$
$$= cV_\infty \sinh\xi \cos\eta \qquad (1)$$

is added to that given in Ref. 6., then the velocity potential for the streaming motion past the ellipsoid is given by

$$\Phi = (-c/k)V_\infty[1 - \sinh\xi \cot^{-1}\sinh\xi - k\sinh\xi]\cos\eta \qquad (2)$$

The potential function given by Eq. (2) can be shown to satisfy the conditions of continuity and irrotationality of the flow plus the usual boundary conditions that at infinity the uniform flow is undisturbed by the presence of the body in the stream, and at the surface of the ellipsoid the normal components of the fluid velocity are zero.

The flowfield velocity (V) can now be determined by recalling that

$$V^2 f'(\zeta)\bar{f}'(\bar{\zeta}) = (\partial\Phi/\partial\eta)^2 + (\partial\Phi/\partial\xi)^2 \qquad (3)$$

Evaluation of the functions $f'(\zeta)\bar{f}'(\bar{\zeta})$, $\partial\Phi/\partial\eta$, $\partial\Phi/\partial\xi$ and their substitution into Eq. (3) gives the normalized velocity distribution as

$$(V/V_\infty) = [k^2(\sinh^2\xi + \cos^2\eta)]^{-1/2}[(1 - \sinh\xi \times \cot^{-1}\sinh\xi - k\sinh\xi)^2 \sin^2\eta + (\tanh\xi - \cosh\xi\cot^{-1} \times \sinh\xi - k\cosh\xi)^2\cos^2\eta]^{1/2} \qquad (4)$$

where V/V_∞ is a function of b/a and of x.

If we set $\xi = \xi_0$ in Eq. (4); for example

$$\xi = \xi_0(1/2)\ln[(1 + b/a)/(1 - b/a)] \qquad (5)$$

then we get an expression for the normalized velocity distribu-

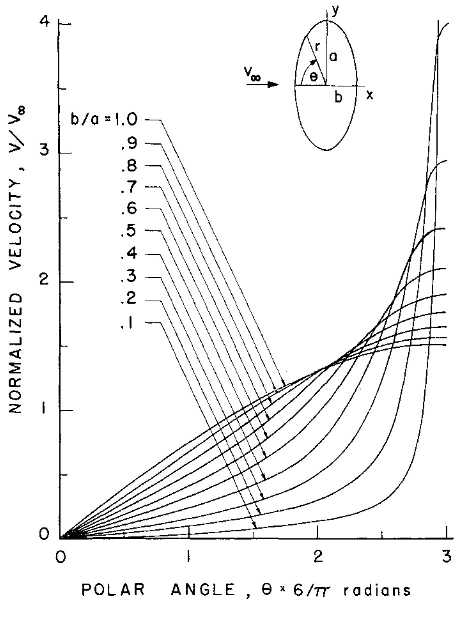

Fig. 1 Normalized velocity distribution vs polar angle for the flow around a planetary ellipsoid.

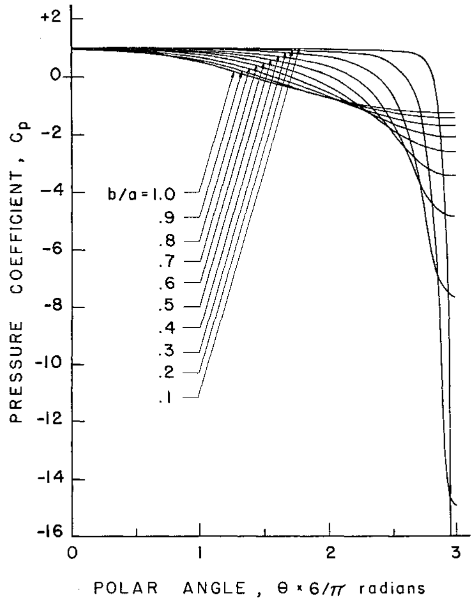

Fig. 2 Pressure coefficient vs polar angle for the flow around a planetary ellipsoid.

tion at the surface of the body. The ratio of the semiminor axis (b) to the semimajor axis (a) is referred to as the eccentricity parameter and its magnitude is an indication of the degree to which the body of revolution deviates from that of a sphere. For example, if we set b/a equal to unity, then Eq. 4 gives the velocity distribution over the surface of a sphere; whereas, if we set b/a equal to zero, we obtain the solution for the flow over a round disk of radius a.

The evaluation of Eq. (4) over the surface of the body, for various values of the eccentricity parameter ($0 \leq b/a \leq 1$), is facilitated by transforming the cartesian coordinates (x,y), of the points describing the ellipse $\xi = \xi_0$, into polar coordinates (r,θ). The main advantage to be realized through this manipulation is that the solution for V/V_∞ can be obtained as a function of θ rather than of x. A polar coordinate transformation gives

$$x^2 = b^2/[1 + (b/a)^2\tan^2\theta] \qquad (6)$$

which is then used to write relationships for $\sin^2\eta$ and $\cos^2\eta$ as

$$\sin^2\eta = 1 - (b/a)^2/[1 + (b/a)^2\tan^2\theta][1 - (b/a)^2]\sinh^2\xi_0 \qquad (7a)$$

$$\cos^2\eta = (b/a)^2/[1 + (b/a)^2\tan^2\theta][1 - (b/a)^2]\sinh^2\xi_0 \qquad (7b)$$

Substitution of Eq. (7) into Eq. (4) then gives V/V_∞ as a function of the parameter b/a and the polar angle θ.

Finally, with the velocity having been found, the pressure distribution over the surface of the body can be obtained from Bernoulli's equation for an ideal fluid. The normalized pressure distribution or pressure coefficient, C_p, is, from Bernoulli's equation, given by

$$(p - p_\infty)/(\tfrac{1}{2}\rho_\infty V_\infty^2) = 1 - (V/V_\infty)^2_{\xi = \xi_0} \qquad (8)$$

where $p = p(\theta,b/a)$ is the static pressure on the ellipsoidal surface, and p_∞ is the undisturbed static pressure in the fluid at a point far from the body.

Discussion of Results

The results of a parametric evaluation of the velocity distribution and pressure coefficient are shown, respectively, in Fig. 1 and Fig. 2 where V/V_∞ and C_p are both plotted as a function of the polar angle θ with the eccentricity b/a as a parameter. Since these distributions are symmetric with respect to the equatorial axis, the solutions are shown only for $0 \leq \theta \leq \pi/2$. As one would expect, in the limit as $b/a \rightarrow 1$, the distributions of velocity and pressure are seen to approach those for the case of a sphere in an ideal fluid. But as $b/a \rightarrow 0$, i.e. as the drop is flattened out by the aerodynamic forces in a direction perpendicular to that of the undisturbed flow, the velocity and pressure are seen to deviate considerably from those of a sphere. For example, a typical empirical value[5] of the eccentricity parameter, corresponding to the condition of maximum droplet diameter, is $b/a \simeq 0.35$.

The general observation can be made that drop flattening has the dual effect of reducing the magnitude of the flow velocity over much of the windward surface while at the same time increasing the fluid velocity in the region of the equator. It is felt that the significant increase in shearing velocity near the equator is an important contributing factor in the high-speed aerodynamic breakup of liquid droplets. In other words, it is apparent that, by virtue of the droplet deformation or flattening, a high shearing velocity is generated in the vicinity of the equator, which hastens the disintegration process by enhancing the boundary-layer stripping of liquid away from the droplet equatorial surface. Also, the reduction of flow velocity over a large portion of the windward surface has the effect of producing an extensive quasi-stagnation region, as shown in Fig. 2, and the extent of this region is seen to depend on the magnitude of b/a. Hence, the pressure coefficient over much of the surface is positive ($C_p \geq 0$), the manifestation of which is a higher drag force than otherwise would exist if the droplet shape remained spherical. Since Taylor's model does not account for either of these important effects, it seems reasonable to conclude that it will give conservative results for liquid droplet acceleration and disintegration rate in a high-speed gas stream.

References

1 Batchelor, G. K. and Davies, R. M., eds., "The Mechanics of Drops and Bubbles," *Surveys in Mechanics*, Cambridge University Press, 1956, pp. 162–215.

2 Hinze, J. O., "Fundamentals of the Hydrodynamic Mechanism of Splitting in Dispersion Processes," *AIChE Journal*, Vol. 1, No. 3, Sept. 1955, pp. 289–295.

3 Hanson, A. R., Domich, E. G., and Adams, H. S., "Shock Tube Investigation of the Breakup of Drops by Air Blast," *The Physics of Fluids*, Vol. 6, No. 8, Aug. 1963, pp. 1070–1080.

4 Batchelor, G. K., ed., "The Shape and Acceleration of a Drop in a High Speed Air Stream," *The Scientific Papers of G. I. Taylor*, Vol. III, Cambridge University Press, 1963, pp. 457–464.

5 Ranger, A. A. and Nicholls, J. A., "The Aerodynamic Shattering of Liquid Drops," *AIAA Journal*, Vol. 7, No. 2, Feb. 1969, pp. 285–290.

6 Milne-Thomson, L. M., *Theoretical Hydrodynamics*, 3rd ed., Macmillan, New York, 1955, pp. 453–455.

Nonequilibrium in an Arc Constrictor

Frank P. Incropera*

Purdue University, Lafayette, Ind.

and

John R. Viegas†

NASA Ames Research Center, Moffett Field, Calif.

Since the first construction of a cascade arc in which an electrical discharge is confined by the cooled wall of a tube, numerous theories have been developed to predict the associated flow condition. Despite inherent differences, the theories have all had in common the assumption of local equilibrium. In recent years, however, evidence has appeared which suggests that this assumption is inappropriate in regions adjacent to the confining wall.[1,2] The objective of this Note is to obtain a first estimate of the nature and the extent of nonequilibrium in a typical arc. This is done by delineating and uncoupling the effects that influence the equilibrium state of an arc plasma, assigning an appropriate time scale to each effect, and comparing relative magnitudes for typical conditions.

Possible nonequilibrium effects of special interest in an arc include ionization nonequilibrium, nonequipartition of translational energy between electrons and heavy particles, and the existence of an electron velocity distribution function which is non-Maxwellian. At the same time that certain processes act to promote these nonequilibrium effects, competing processes act to restore the corresponding equilibrium condition. For example, the external electric field, thermal conduction, ambipolar diffusion, and inelastic recombination collisions all promote nonequipartition of translational energy. In contrast, electron-heavy particle elastic collisions provide the dominant mechanism for maintaining equipartition. Similarly, the external field and inelastic collisions act to promote a non-Maxwellian electron velocity distribution, while self-collisions in the electron subgas act to restore the equilibrium distribution. Finally, ambipolar diffusion acts to promote ionization nonequilibrium at the same time that ionization or recombination processes act to maintain the corresponding equilibrium condition. In the core of the arc, where diffusion depletes the local electron concentration, the ionization rate must be sufficiently large to maintain an equilibrium electron number density; in the peripheral arc region, diffusion increases the local electron concentration and a sufficient recombination rate is needed to maintain equilibrium.

In this paper the aforementioned equilibrium departure and restoration mechanisms are uncoupled, and each is characterized by an appropriate time scale. Time-scale calculations are then performed using temperature and species concentration profiles obtained from an equilibrium theory for the asymptotic region of a 1 cm diam, atmospheric argon arc.[3] The calculations are performed for arc currents of 35 and 600 amps and provide an approximate estimate of the extent of nonequilibrium in the arc. In addition, a simple treatment of two competing mechanisms is used to illustrate the possible existence of nonequipartition in arcs for a range of operating conditions.

The form of several of the time scales of interest may be obtained from the use of phenomenological arguments in connection with the general relaxation equation

$$\partial Q/\partial t = (1/\tau)(Q^* - Q) \quad (1)$$

where Q may be either a species temperature or concentration and Q^* is generally the corresponding equilibrium value. The so-called equipartition time τ_{eq} is defined as the time required to reach a 67% reduction in some initial electron-heavy particle temperature difference due to elastic electron-atom and electron-ion collisions. To determine this time, the general expression for the random species energy exchange rate in a nonequipartition plasma[4] is used in connection with appropriate gas-kinetic cross sections for electron-ion[5] and electron-atom[6] collisions. Similarly, a characteristic ohmic heating time τ_{oh} may be defined as the time required for the temperature of the electron subgas to be elevated by a factor of e through application of the external field. The electrical conductivity required for the calculations was evaluated using the mixture rule suggested by Kruger and Viegas.[7] The characteristic reaction time τ_r is defined as the time required to achieve a factor of e change in the electron concentration through either collisional ionization or recombination. Since the time-scale calculations are performed using equilibrium temperature and concentration profiles,

Received May 21, 1970. This work was done at NASA Ames Research Center. The work of F. P. Incropera was supported by a summer ASEE-NASA Research Fellowship. This support is gratefully acknowledged.

* Associate Professor of Mechanical Engineering. Member AIAA.

† Research Scientist. Member AIAA.